INFLUENCE AND CONTROL OF BONDLINE THICKNESS IN FUSION BONDED JOINTS OF THERMOPLASTIC COMPOSITES

A. J. Smiley
ICI Composite Structures
Wilmington, DE 19897

and

M. Chao, J. W. Gillespie Jr.
Center for Composite Materials
University of Delaware
Newark, DE 19716

ABSTRACT

The interlayer flow behavior during processing and the strength of fusion bonded thermoplastic composite laminates was investigated. The interlayer flow behavior was modeled as the squeeze flow of a viscous fluid between rigid parallel plates. The results of the model compared favorably with experimental data. It was demonstrated that the bondline thickness can be controlled through the judicious use of glass skrim at the interlayer. The quality of the glass skrim, however, adversely affected the joint strength. In all cases, the joint strength decreased with increased bondline thickness.

INTRODUCTION

The fabrication technology for thermoplastic composite materials has reached a state where individual components can be produced in a cost effective manner. This has been demonstrated on a broad scale with components being produced using processes such as sheet forming, pultrusion, and filament winding [1-3]. Making individual components, however, is only the first step in a truly production viable fabrication process. The next step in producing a structure is the joining and assembly of the separate components. A considerable amount of effort is now being focused on bonding techniques that take advantage of the fusible nature of thermoplastics [4-6]. Some of the key issues in the fusion bonding of thermoplastic composites is part fit-up, the ability of the fusion bonding process to accommodate a certain degree of component mismatch, and the resulting mechanical performance of that joint.

During the fusion bonding of thermoplastic composite laminates the polymer at the bondline interlayer flows to produce intimate contact between adherends and facilitate void migration. It is the characteristics of the interlayer polymer, the processing conditions, and the geometry of the adherends that govern this flow process. The extent of the flow determines the joint bondline thickness, which relates directly to the mechanical

performance of the joint. In addition, poor fit-up of mating parts in a structure can result in bondline thickness variations and therefore poor mechanical performance. The objective of the work described in this paper was; to characterize the effect of process conditions on bondline thickness, to characterize the effect of bondline thickness on the mechanical performance, and to develop a methodology for controlling bondline thickness in fusion bonded thermoplastic composite laminates.

This study employed a dual resin bonding process (Thermabond™) to join carbon fiber reinforced PEEK (APC-2) composite laminates with PEI as the interlayer polymer [7]. Both unreinforced and glass scrim reinforced PEI were utilized at the interlayer. The approach to the stated objective was to initially characterize the flow mechanisms for the different interlayer configurations at the processing conditions employed for bonding. This behavior was modeled using squeeze flow analysis and a bondline thickness predictive capability was developed. The bonded laminates were utilized to experimentally characterize the effect of bondline thickness on mechanical performance. The mechanical performance was characterized by the single lap shear strength and the failure mode of the various joints. The results provide information which is useful in defining the optimum fusion bonding process.

BACKGROUND

Fusion Mechanisms

Prior to the joining process the adherends have resin rich surface layers that do not mate precisely to one another due to variations in the surface. This results in regions of non-contact. During the joining process, sufficient flow must be achieved in the interlayer to fully wet-out the surfaces and allow for migration of entrapped air to produce intimate contact. In addition to intimate contact, good adhesion requires the diffusion of molecules across the bondline interface. Thermal energy input at the bondline during processing must be at a level high enough to produce molecular motion across the interface. These mechanisms, shown schematically in Figure 1, occur at different rates depending on the process conditions.

Thermabond™ Process

Thermabond™ is a process that employs an interlayer polymer at the bonding surface with different characteristics than the reinforced polymer in the composite. Fusion between this interlayer polymer and the reinforced polymer is essential in order to obtain optimum

properties. Therefore the interlayer polymer should be compatible, at the molecular level, with the polymer matrix employed in the composite.

Fusion of the interlayer polymer and the composite laminate is achieved during the consolidation of the composite component. A layer of the interlayer polymer film (typically 75 μm thick) is placed on the composite laminate in the area's to be bonded prior to consolidation. During consolidation both polymers are in the molten state and molecular diffusion and blending occurs creating a bond between the two polymers. Upon cooling the composite component is left with a thin layer of the interlayer polymer on the bonding surfaces.

Joining is performed by bringing the components together (optionally additional interlayer polymer is placed in the bondline to fill any irregularities between the two surfaces to be mated) and applying sufficient force to bring the mating surfaces and the interlayer into conformance. The interlayer is then heated sufficiently above its glass transition temperature to allow it to fuse throughout, but not sufficiently to melt the matrix of the composite laminate. The system is then cooled below the glass transition temperature of the interlayer resin while maintaining the clamping force to complete the bonding process.

A good example of a Thermabond™ system, and the one employed in this study, is an Aromatic Polymer Composite (APC-2) made from 61% by volume carbon fiber reinforced polyether etherketone (PEEK) as the structural composite and an amorphous polyetherimide (PEI) resin as the thermoplastic interlayer. The relative physical characteristics of these two polymers are illustrated in Figure 2. The polyether etherketone is a semi-crystalline polymer having a glass transition temperature, T_g, of 140°C and a melting point of 340°C. The amorphous polyetherimide has a glass transition temperature of 210°C. This dual polymer system facilitates bonding at temperatures between 260°C and 315°C. Below 260°C a suboptimal bond will be formed due lack of flow in the high-viscosity PEI interlayer. Above 315°C, softening in the PEEK composite matrix polymer can cause the structural composite to distort. Further details on this process can be found in the literature [7].

EXPERIMENTAL PROCEDURES

Fusion bond strength is dependent upon the mechanical properties and the geometry of the bondline interlayer. The final bondline thickness is a function of the flow at the bond

interlayer during processing. This flow is driven by the processing history (temperature and pressure), the interlayer material properties, and the initial geometry of the interlayer. The objective of the experimental work performed was to characterize the interlayer flow behavior and the bond strength for single lap joints produced using different interlayer configurations and processing conditions. This section describes the test matrix and the panel and bonding processing procedures.

Test Matrix

Different interlayer configurations which consisted of various combinations of neat PEI polymer film and glass/PEI skrim were examined in this study. The neat PEI is a relatively low viscosity material that flows readily which facilitates interlayer surface wetting and void migration. It is possible however, to produce too much flow that could result in a less than optimum bondline thickness or insufficient wetting in laminates with high surface mismatch. Therefore, the use of a PEI impregnated glass skrim (67% fiber volume fraction, 0.127 mm thickness) was investigated as a method for controlling the flow. The interlayer configurations employed were based on the material combination and the initial bondline thickness. There were three different material configurations used including; neat PEI, all glass skrim, and hybrids of alternating layers of PEI and glass skrim. There were also three initial thicknesses employed; 0.127, 0.0635, and 0.0254 cm. All panels were bonded under identical processing conditions (see bonding procedures) with the exception of two. The addition two panels had initial neat PEI interlayers 0.127 cm thick. These panels were processed for shorter dwell times in order to identify the effect of process conditions on the resulting bondline thickness.

Panel Processing

The laminates employed in this study consisted of 16 ply quasi-isotropic $[0/45/90/-45]_{2s}$, APC-2/AS4 material. They were autoclave consolidated with 0.0127 cm layers of PEI (Ultem 1000) film on the top and bottom surface. A typical vacuum bag assembly, shown schematically in Figure 3, consisted of a Upilex "R" bag with 7781 fiberglass breather and a steel caul plate, all coated (except the fiberglass) with Frekote FRP mold release agent.

The panel processing cycles were carried out with full vacuum (>711 mm Hg) throughout. A pressure of 0.138 MPa was applied prior to ramping up the temperature. The temperature was then increased to 391 °C ± 9 °C. When the temperature was within 15 °C of the set point (391 °C), a pressure of 0.689 MPa was applied. The panel was held at 391 °C and 0.689 MPa for 30 minutes. The autoclave was then cooled and when the

temperature went under the T_g, 140 °C, the vacuum and autoclave pressure was released. The autoclave was then allowed to cool to room temperature and the panels were removed. The fully consolidated panels were then trimmed to produce the 16.5 cm by 10.2 cm laminates required for bonding.

Bonding Procedures

Prior to bonding, acetone was used to clean the panels and remove any impurities on the surface as a result of prior handling. In addition, the panels and all the interlayer materials (PEI film and Glass/PEI skrim) were dried in an oven at 130 °C for 48 hours to eliminate any moisture that could produce voids during bonding. Fusion bonding of the APC-2/PEI panels was performed in a hot press utilizing an aluminum fixture to ensure proper alignment of the final part. The bonding stack assembly, shown in Figure 4, consisted of the two laminates aligned in the fixture to produce a 1.27 cm overlap. The interlayer material (PEI film and glass/PEI skrim) was placed at the bond interface. An aluminum pressure plate was placed over the laminates and the whole assembly was vacuum bagged and placed in a hot press. The hot press was employed only to provide heat. The 200 psi bonding pressure employed was created by the transfer of vacuum pressure by the large pressure plate to the smaller area of the bondline. Once the assembly was placed in the press, and the pressure was applied, the system was heated up to 250 °C and held at this temperature for 30 minutes. The assembly was then removed from the press and quenched in a cold water bath. The processing history was monitored with three thermocouples placed directly at the bondline and a pressure transducer in the vacuum line using National Instruments computer based LabView data acquisition system [8]. Typical data from a bonding processing run is shown in Figure 5.

INTERLAYER FLOW CHARACTERIZATION

Squeeze Flow Analysis

In this paper, the squeeze flow of an incompressible viscous fluid of arbitrary thickness between two rigid parallel rectangular plates is employed to model the interlayer flow during fusion bonding. The objective of the model is to predict the transient bondline thickness as a function of the processing history.

The squeeze flow analysis described herein was based on similar work performed for thermoset adhesives [9]. The analysis domain, illustrated in Figure 6, is a 2D Cartesian system on X and Z. Using symmetry, this domain is defined by the half length of the

overlap, $X_o/2$, and the transient bondline thickness, $b_{lt}(t)$. The flow is driven by a constant applied pressure, P_a, on the upper plate. The assumptions employed in the model development are as follows; Newtonian fluid behavior, Quasisteady-state (Creeping) flow, and the bondline is very thin relative to it's length, hence any pressure gradients through the thickness are neglected, (P=P(x) only). Employing these assumptions along with the x-momentum equation yield's the Reynold's Lubrication equation:

$$\frac{\partial P}{\partial X} = \eta \frac{\partial v_x^2}{\partial^2 Z} \tag{1}$$

where, P is the pressure in the fluid, η is the fluid viscosity, and vx is the flow velocity in the x-direction. The system boundary conditions include the following; A no slip condition at the panel surfaces;

$$v_x = 0 \quad \text{at} \quad Z = 0 \text{ and } Z = b_{lt}(t), \tag{2}$$

symmetry condition at the centerline;

$$V_x = 0 \quad \text{at} \quad X = 0, \tag{3}$$

vacuum pressure, P_o, at the free surface;

$$P = P_o \quad \text{at} \quad X = X_o/2, \tag{4}$$

and a constant external pressure force on the upper panel;

$$F_e = P_a X_o w \quad \text{at} \quad Z = Zo, \tag{5}$$

where w is the width of the flow domain. The initial condition is based on the initial thickness of the interlayer;

$$b_{lt}(t) = Zo \quad \text{at} \quad t = 0. \tag{6}$$

Integration of equation (1) and applying the boundary conditions yields an equation relating the x-velocity to the pressure gradient. This can be combined with the conservation of volume and force equilibrium equations to yield an expression for the bondline thickness, Z(t), as a function of the process parameters. This equation, shown below, requires a time

$$b_{lt}(t) = \sqrt{\left\{\int_0^t \frac{1}{\eta}\, dt * \left[\frac{2(P_a - P_o)}{X_o^2}\right] + \frac{1}{Z_o^2}\right\}^{-1}} \tag{7}$$

integration that involves the viscosity. The bonding process is non-isothermal and therefore the viscosity term varies with time through the temperature. The temperature

dependent viscosity of the interlayer is modeled by a modified Arrhenius equation as shown below.

$$\eta(T) = A\,EXP\left(\frac{B}{(T-T_g)}\right) \tag{8}$$

The above equation was fitted to experimental data for PEI to obtain the constants A=1074 poise and B=435 (see Figure 7). Therefore, by knowing the processing history, the material properties, and the initial bondline configuration; the bondline thickness, Z(t), can be calculated as a function of time.

A computer program was employed to compute the transient bondline thickness of a neat PEI interlayer for the bonding conditions previously shown in Figure 5. The analysis results, shown in Figure 8, illustrate the nature of the flow and the effect of pressure. Initially there is no flow because the temperature is below the glass transition, T_g, and the viscosity is still very high. Above T_g, the polymer begins to soften which initiates the flow and the bondline thickness decreases steadily with time. As the bondline thickness decreases the driving force for the flow decreases due to dynamic equilibrium. Thus, an apparent asymptotic bondline thickness is reached over the dwell time of interest. As would be expected, decreasing the applied pressure, Pa, slows the flow. This reduces the rate at which the bondline thickness decreases and increases the asymptotic bondline thickness.

A similar analysis is performed for the hybrid interlayer. The hybrid interlayer consists of alternating layers of glass skrim reinforced polymer and polymer film. This multi-layer system, shown schematically in Figure 9, consists of multiple flow domains. The lack of a pressure gradient through the thickness can be extended to the assumption in this case that there is no flow through the glass skrim. Therefore, each individual flow domain behaves independently and can be analyzed as such. It follows that the analysis based on equation (8) can be applied directly and the transient bondline thickness for a hybrid interlayer is simply the sum of the transient behavior of each flow domain and the constant thickness of the skrim layers.

The predicted flow behavior of several different hybrid interlayers is shown in Figure 10. The nature of the flow is similar to the neat polymer case previously described. The rate of the decrease in bondline thickness, however, is much slower. This is due to the much thinner flow domains. As expected, increasing the number of skrim layers reduces the

flow rate and the thickness decrease. An asymptotic thickness is again reached, however, the difference in the asymptotic thickness predictions is due to the differing number of constant thickness skrim layers. The predicted bondline thickness results for the neat PEI and the hybrid interlayers will be compared with actual bonded panels later in this paper.

Experimental Characterization

The bonded composite laminates were cut with a water cooled diamond saw to yield four-2.54 cm by 17.5 cm single lap shear samples and seven bondline thickness characterization specimen. The locations of the cuts are shown in Figure 11. The bondline thickness characterization specimen were mounted in an epoxy resin and polished to a clear finish. Photomicrographs of each specimen were taken at magnifications from 60x to 100x depending upon the thickness of the specimen. Measurement of bondline thickness was performed directly from the photomicrograph. Due to fiber flow near the bondline, a reference for the measurements was defined at the ply interface two layers away from the bondline. The final bondline thickness, b_{lt}, is defined as the distance between the reference lines minus the thickness of 4 plys as shown in equation (9). The ply thickness is also measured from the photomicrograph for each sample. Figure 12 shows the typical location of the reference lines on a photomicrograph.

$$b_{lt} = b_{meas} - 4(\text{Ply Thickness}) \qquad (9)$$

The interlayer flow behavior was characterized by microscopic inspection and thickness measurements of the final bondline area of each specimen. The transient flow behavior of the neat PEI interlayer was obtained through inspection of panels bonded at different dwell times. The series of photomicrographs in Figure 13 show that, not surprisingly, the amount of flow increases with dwell time. The micrograph in Figure 13(d) shows the "spew" created at the edge of the overlap due to the flow. Naturally, since the flow increases with time, the bondline thickness decreases with time as indicated by the data in Table 1. This data, which includes results from all of the specimens with a neat PEI interlayer, also shows that an asymptotic bondline thickness is obtained experimentally for long dwell times independent of the initial bondline thickness. The graph in Figure 14 illustrates that the experimental results compare favorably with the predicted behavior. The difference in the rate of thickness decrease between the predicted and the actual behavior could be due to an under estimation of the flow viscosity or a lack of accounting for the effect of the "spew" on the bondline flow behavior. The effect of the "spew" would be to increase the back pressure at the exit of the flow domain, thus slowing the flow and

increasing the asymptotic thickness. This should be included in further refinements of the squeeze flow model.

The use of layers of glass skrim in the interlayer has a tendency to slow the flow. This is illustrated by comparison of the bondline area micrographs in Figures 13(d) and 15. The former is the neat PEI interlayer and the latter is a hybrid interlayer created with 6 layers of 0.0127 cm thick PEI film and 5 layers of 0.0127 cm thick glass skrim. Although the initial thickness of each interlayer was the same, the hybrid interlayer did not flow as much. Further evidence of this effect is the bondline thickness results shown in Figure 16. The processing cycles were identical for all the specimen employed in producing this data. The results indicate that for the neat PEI interlayer the final bondline thickness is independent of initial thickness for the 30 minute dwell time employed. The final bondline thickness of the hybrid interlayer specimen is dependent upon the amount of glass skrim employed. Finally, there is effectively no flow in the all skrim interlayer as evidenced by the little change between the initial and final bondline thickness.

Comparison of the hybrid interlayer results with the predicted behavior is shown in Table 2. The results shown in the Table indicate that excellent agreement is obtained between the predicted thickness and measured thickness. These results however, are the final bondline thickness of specimen bonded with a relatively long dwell time. A better indication of the accuracy of the model would be data for shorter dwell times.

MECHANICAL PERFORMANCE CHARACTERIZATION

Single Lap Shear Test

The mechanical characterization was performed using the single lap shear test based on the ASTM D1002 specification. The testing was carried out on a 1125 Instron at a cross head speed of 0.05 in/min . The specimen geometry, shown in Figure 17, included a total length of 17.5 cm, a gage length of 10.0 cm, a width of 2.54 cm and an overlap length of 1.27 cm. The coupon was held 3.75 cm into the friction grip. The samples were tested at room temperature with a relative humidity of 50 %. The strength, σ_{SLS}, was calculated as the failure load divided by the overlap bond area.

Several investigators have analyzed the stress distribution in the single lap shear specimen [10-12]. A schematic illustration of the typical stress distribution in the adhesive of a loaded single lap shear specimen is shown in Figure 18. There are stress concentrations at

the end of the joint overlap in both the shear and the peel stresses. The peel stresses are produced as a result of the eccentricity of the single lap specimen. These peel stresses are dependent upon the bondline geometry (overlap length and thickness) and can be large enough to cause failure in peel instead of shear. Thus, when employing the single lap shear specimen, it is just as important to characterize the failure mode as it is to characterize the failure stress.

The types of failure modes expected in this study are shown in Figure 19. The first is cohesive failure which can be produced by failure of the adhesive in shear or peel. A detailed SEM analysis of the fracture should reveal the type of stress that caused the failure. The second mode is adhesive failure which is produced by a lack of adhesion between the adhesive and the adherend. This type of failure would result in a relatively smooth and clean fracture surface on the adherend. The final failure mode considered is the interlaminar failure. This will only occur in a laminated adherend. It is caused by the high peel stresses in the sample reacting on a laminated structure with a relatively low interlaminar strength. If an interlaminar failure is produced, then the adhesive was not loaded to it's fullest capacity.

Results and Discussion

As stated earlier, all the panels bonded were employed to make single lap shear test specimen. This resulted in specimen with various interlayer configurations and bondline thicknesses. The strength results for all the panels tested are shown graphically as a function of bondline thickness in Figure 20.

The strength results indicate that in general joint strength decreases with increased bondline thickness. This is consistent with other published results [13]. The effect of the bondline thickness on strength could be due to changes in; the plastic deformation of the interlayer, the residual stress distribution, and the sensitivity to defects. The neat PEI interlayer specimen with the thin bondlines (0.02 to 0.04 cm) failed in the interlaminar mode as shown in Figure 21. There is a significant variation in the strength of these samples. The only noticeable difference between them is the size of the "spew" at the edge of the overlap. The larger the "spew", the lower the bond strength. It is possible that the spew is creating additional stress concentration.

The strength results for the hybrids and the all skrim interlayer were lower than the strength of the neat PEI interlayer samples. The use of the glass skrim will cause the interlayer to

behave in a more brittle fashion which may explain the lower strength. In addition, the skrim used in these samples was not optimized for mechanical properties. The samples that contained the glass skrim failed in the interlayer leaving a significant amount of exposed glass fibers as shown in Figure 21. Before any real assessment of strength can be made for joints with this type of interlayer geometry, the skrim material should be improved.

SUMMARY AND CONCLUSIONS

This paper describes work performed to study the bondline thickness effects in fusion bonded thermoplastic composite laminates. The approach was to study the flow characteristics of the bondline interlayer and the influence of the bondline geometry on the joint strength.

The interlayer flow behavior was modeled using a squeeze flow analysis. Comparison of the model with experimental data for a neat resin interlayer showed that the model accurately predicted the nature of the interlayer flow, but over predicted the rate and the amount of flow that would take place. A further refinement to the model that would include the effect of the "spew", created by excess resin flow, should increase the accuracy of the model. The bondline thickness results showed that an asymptotic thickness was obtained in the neat resin samples independent of the initial bondline thickness. This illustrates the need for an interlayer methodology that can be used to control the final thickness.

The use of glass skrim was investigated as a technique for controlling the final bondline thickness. The glass skrim had a tendency to slow the flow during processing. This was verified in the model and the experimental results. It was shown that by employing various combinations of neat PEI film and glass skrim at the interlayer, one could produce a range of bondline thicknesses. The squeeze flow analysis modified to model the hybrid interlayer accurately predicted the final bondline thickness of several different interlayer configurations. This demonstrates that the flow model could be employed to determine the optimum processing conditions and interlayer geometry for a desired range of bondline thicknesses.

The mechanical performance characterization indicated that the bondline thickness can greatly affect the joint strength. In the range of thicknesses considered for the neat PEI interlayer, the joint strength decreased 27% from 48 to 35 MPa. In addition, the results

showed that the use of glass skrim at the interlayer adversely affects the joint strength. This was due to the poor mechanical properties of the the glass skrim material.

This work will continue in the future with a focus on optimizing and extending the use of the skrim interlayer system. The ability of the hybrid interlayer to self adjust to thickness variations due to component mismatch will be investigated. Further refinements to the squeeze flow model will aid this activity. The mechanical performance of the glass skrim will be investigated and improved so as not to adversely affect the joint strength. Once a viable system is developed it will be employed in the joining of structural components for verification.

REFERENCES

1. R. B. Ostrom, S. B. Koch, and D. L. Wirz-Safranek, 34th International SAMPE Symposium, pp. 300-311 (1989)
2. S. R. Taylor and W. M. Thomas, 22nd International SAMPE Technical Conference, pp. 78-87 (1990)
3. M. Cirino, T. P. Watson, and D. E. Hauber, 36th International SAMPE Symposium, pp. 2184-2196 (1991)
4. A. Benatar and T. G. Gutowski, *SAMPE J.*, **23**, 33 (1987)
5. M. N. Watson,'Techniques for Joining Thermoplastic Composites', The Welding Institute, Abington, Cambridge, UK.
6. E. M. Silverman and R. A. Griese, *SAMPE J.*, **25**, no. 5, (Sept./Oct. 1989).
7. A. J. Smiley, A. Halbritter, F. N. Cogswell and P. J. Meakin, *Polymer Eng. Sci. J.*, **31**, No. 7, (1991).
8. LabView User's Manual, National Instruments Co., Austin, Texas, (1991).
9. T. M. Donnellan, J. G. Williams and R. E. Trabocco, 15th National SAMPE Technical Conference, pp. 478-488 (1983).
10. M. Goland and E. Reissner, *J. App. Mechanics*, Vol. 11, pp. A17-A27 (1944).
11. L. J. Hart-Smith, NASA CR-112236, Jan. 1973.
12. I. U. Ojalvo and H. L. Eidinoff, *AIAA J.*, Vol. 16, No. 3, pp. 204-211 (1978).
13. A. J. Kinloch, Adhesion and Adhesives - Science and Technology, Chapman and Hall (1987) Chpt. 6, pp. 188-259.

FIGURES

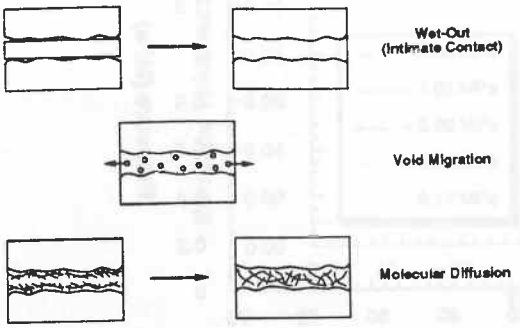

Figure 1. - Adhesion Mechanisms.

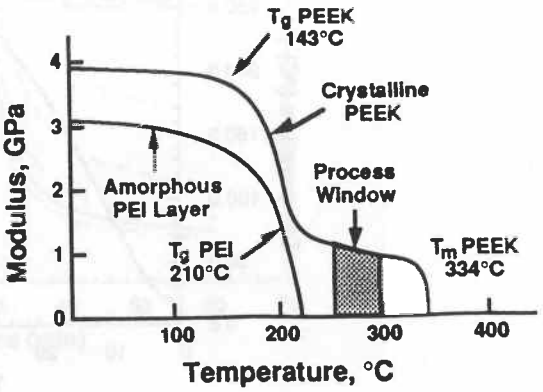

Figure 2. - Physical Characteristics of PEEK and PEI.

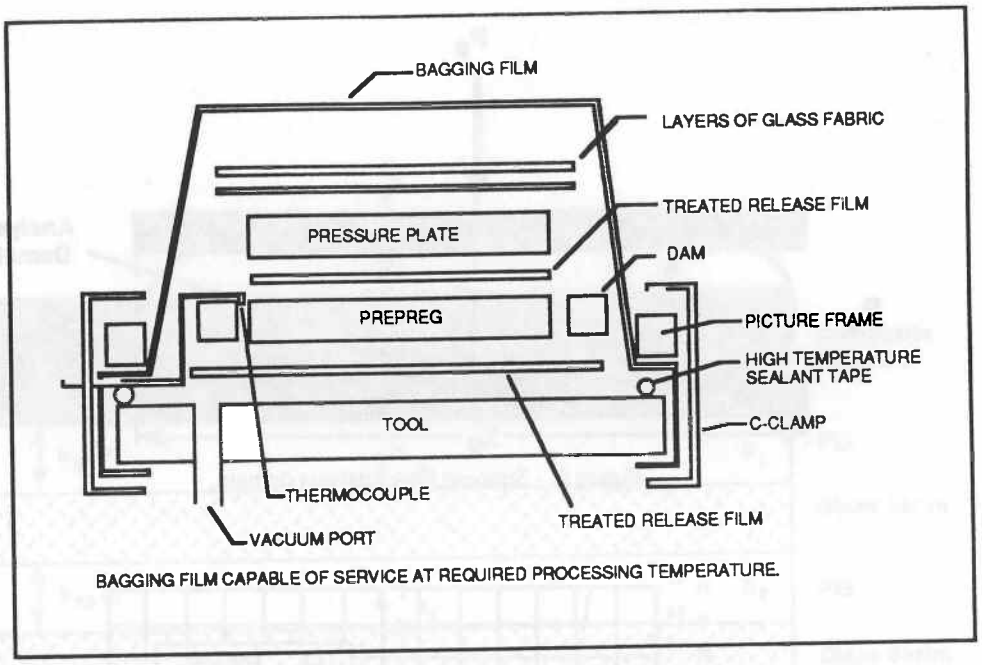

Figure 3. - Typical Vacuum Bag Assembly.

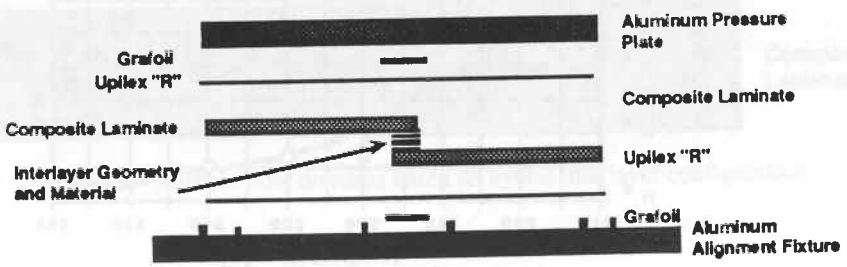

Figure 4. - Bonding Stack Assembly.

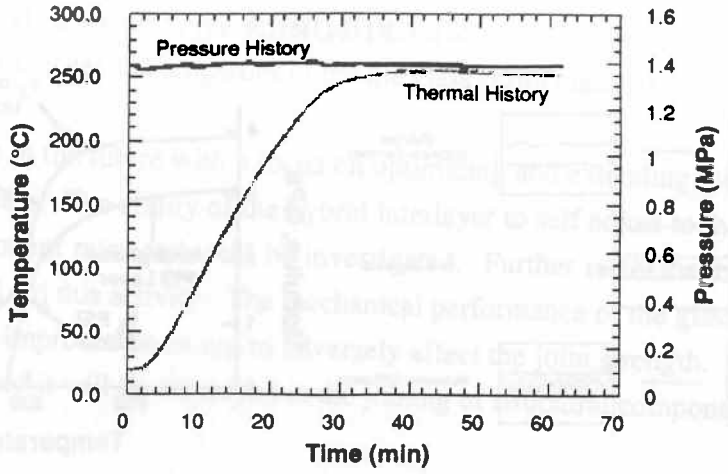

Figure 5. - Processing data acquired during a typical bonding cycle.

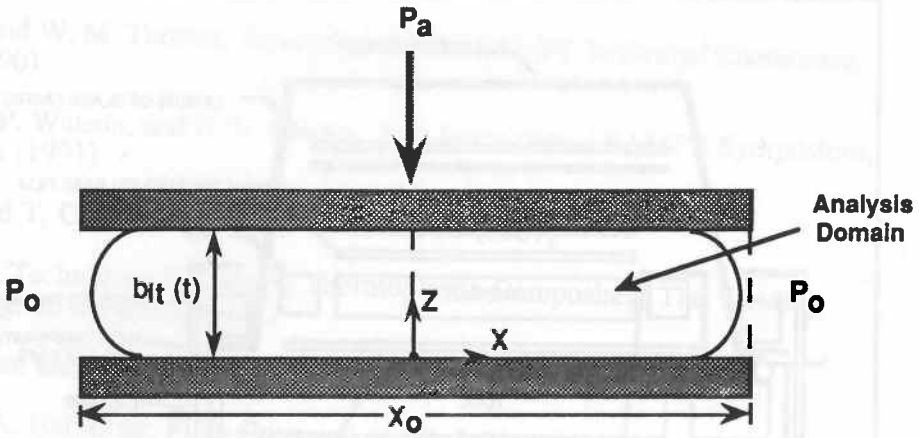

Figure 6. - Squeeze flow analysis domain.

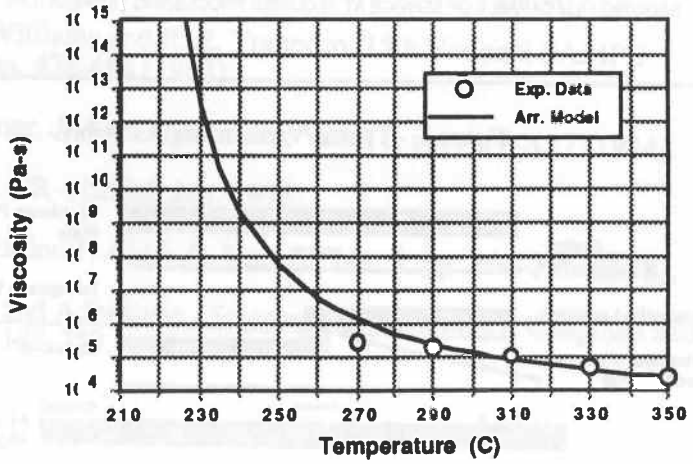

Figure 7. - Arrhenius model of temperature dependant viscosity.

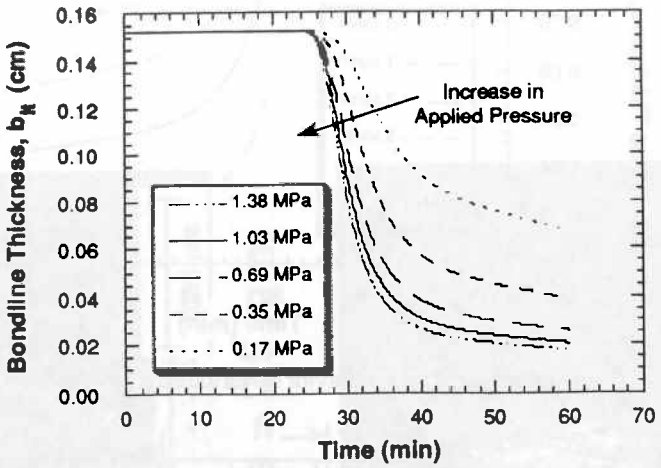

Figure 8. - Predicted transient flow behavior for neat PEI interlayer.

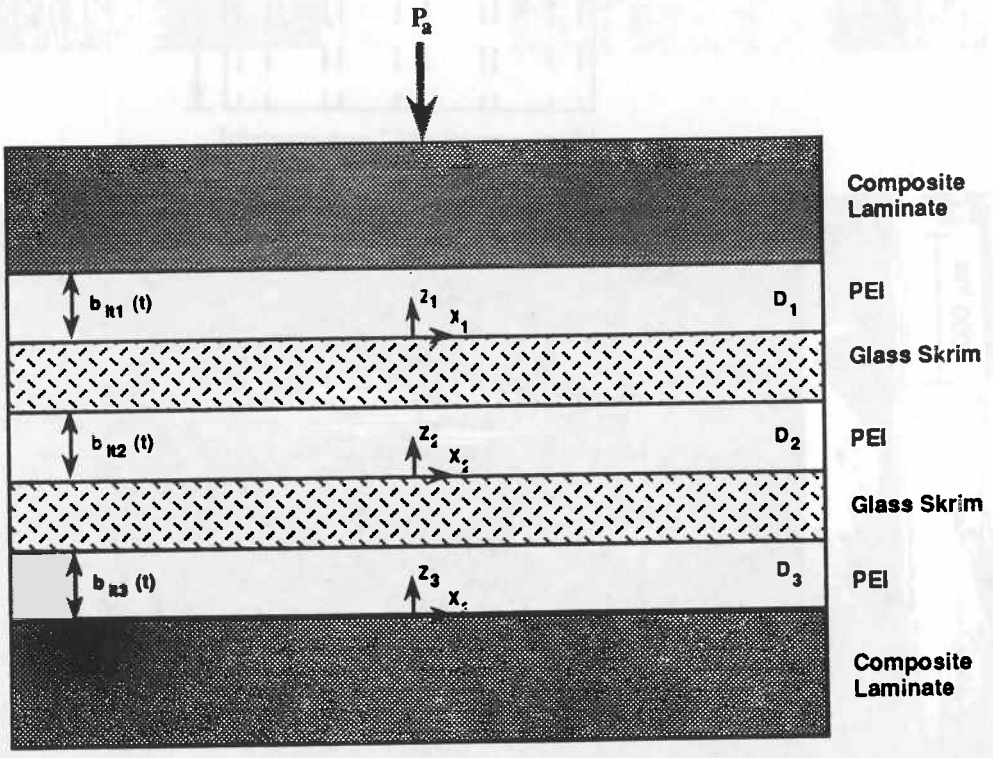

Figure 9. - Mutiple flow domains based on hybrid interlayer configuration.

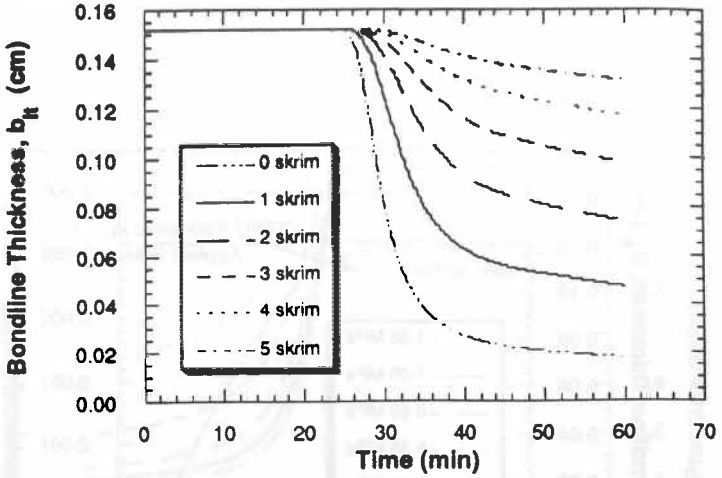

Figure 10. - Predicted transient flow behavior of various hybrid interlayer configurations.

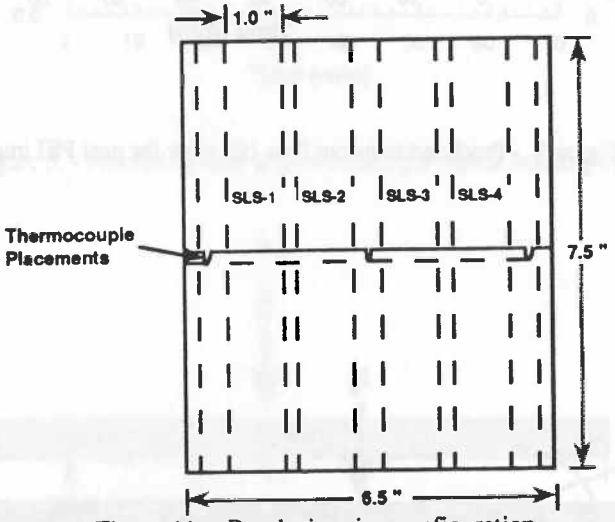

Figure 11. - Panel trimming configuration.

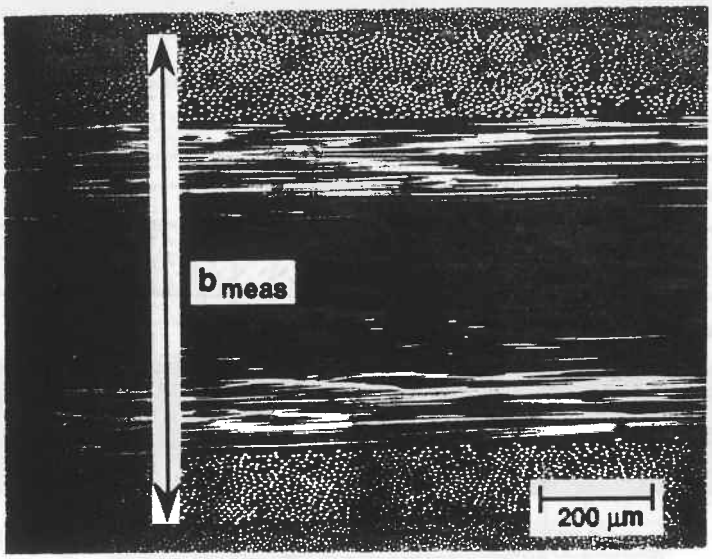

Figure 12. - Ilustration of bondline thickness measurement technique.

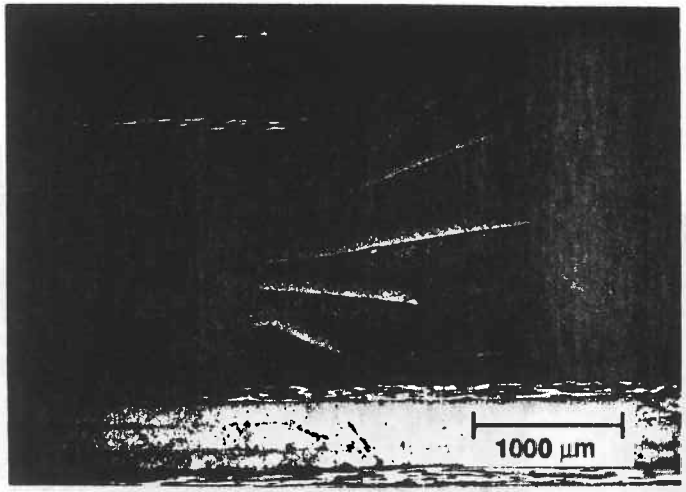

(a) Dwell Time = 0 min.

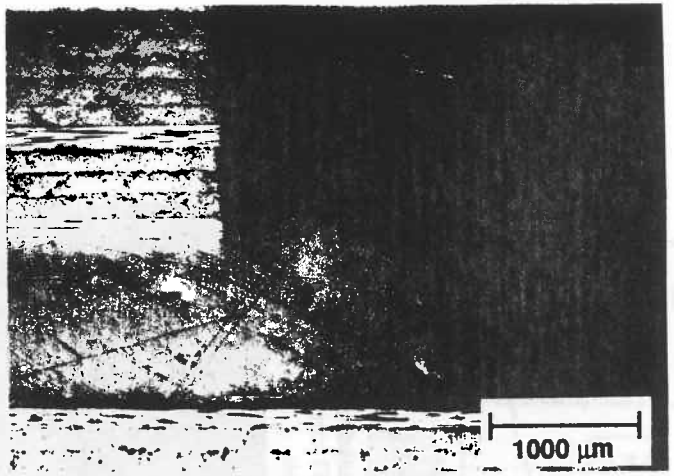

(b) Dwell Time = 2.5 min.

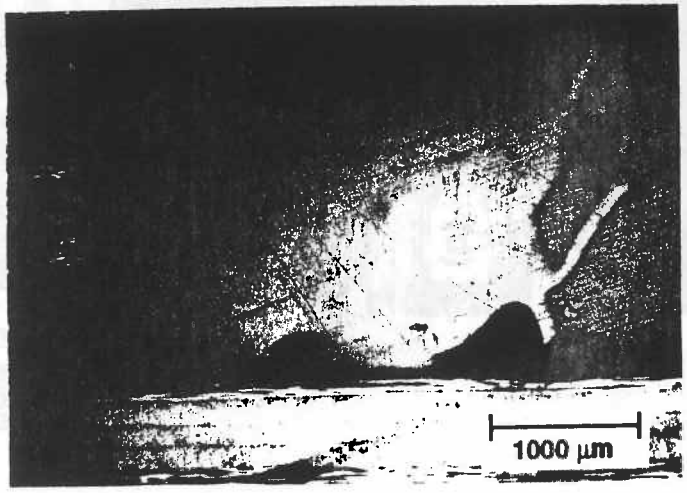

(c) Dwell Time = 5 min.

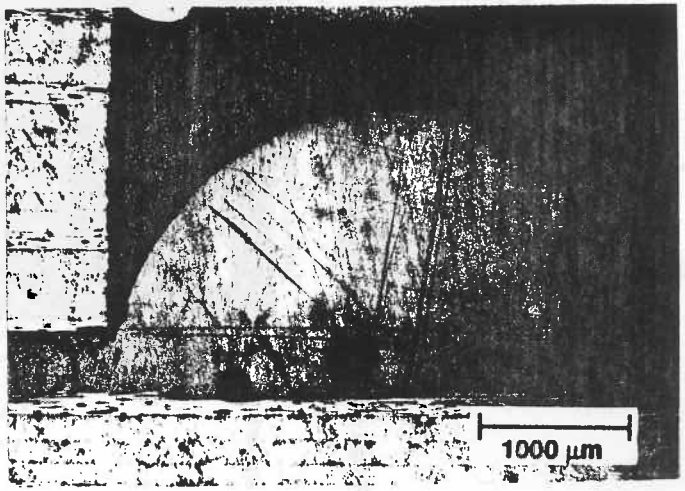

(d) Dwell Time = 30 min.

Figure 13 - Transient flow behavior of neat PEI Interlayer. (Initial bondline thickness of 0.153 cm.)

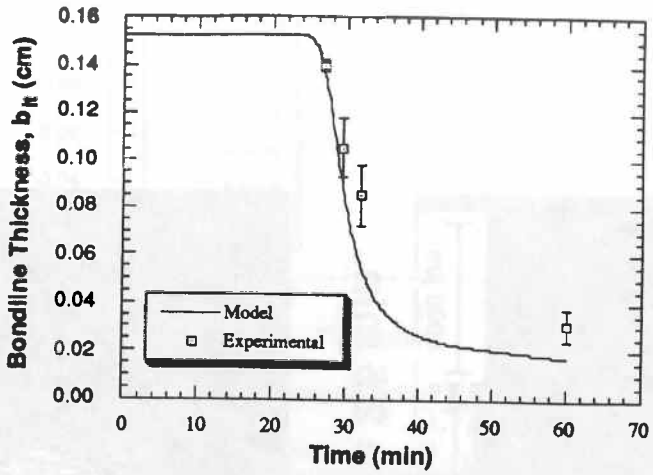

Figure 14. - Comparison of predicted flow and experimental data for a neat PEI interlayer with an initial thickness of 0.153 cm.

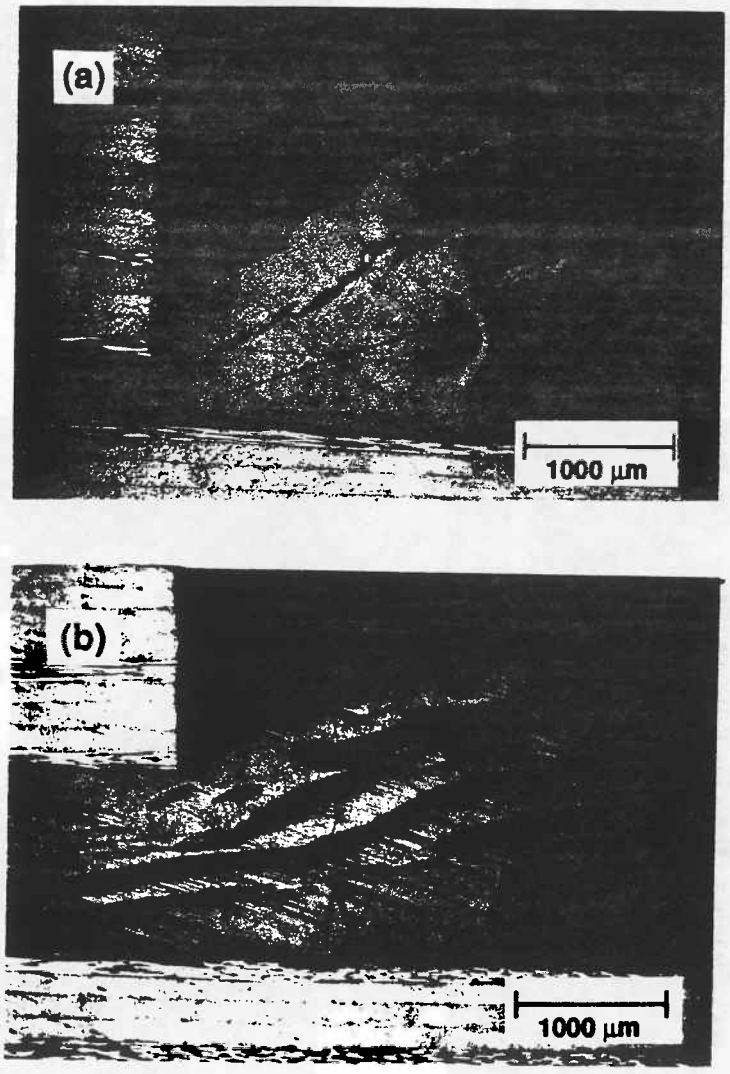

Figure 15. - Photomicrograph illustrating the flow behavior of a hybrid interlayer. (a) 2 layers of PEI, 1 layer of skrim; (b) 6 layers of PEI, 5 layers of skrim.

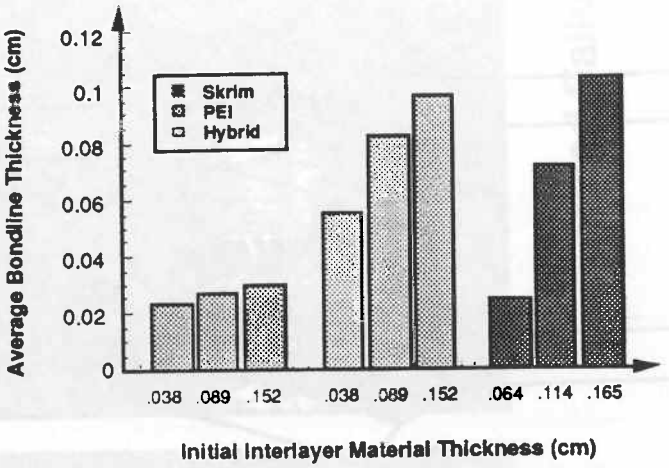

Figure 16. - Compilation of final bondline thickness results for various interlayer configurations. All specimen were processed in identical fashion

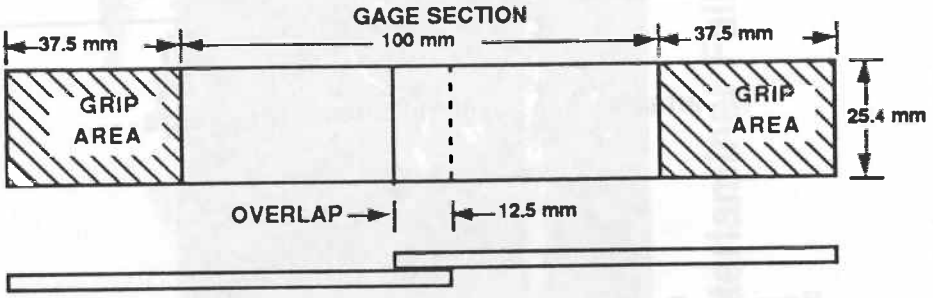

Figure 17. - Single lap shear test specimen geometry.

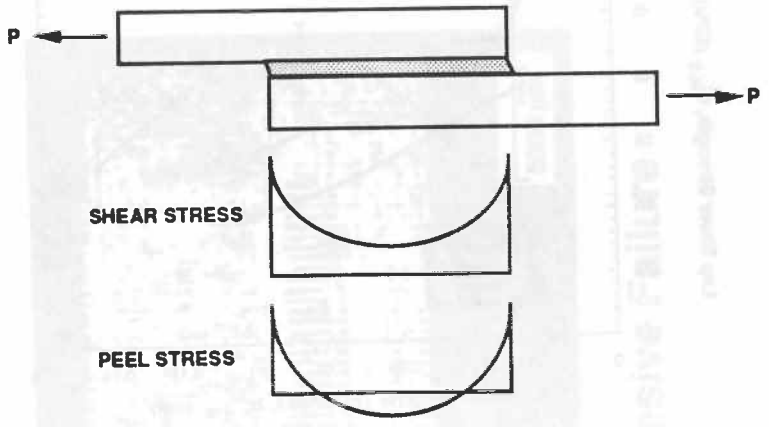

Figure 18. - Adhesive stress distribution in loaded single lap shear specimen.

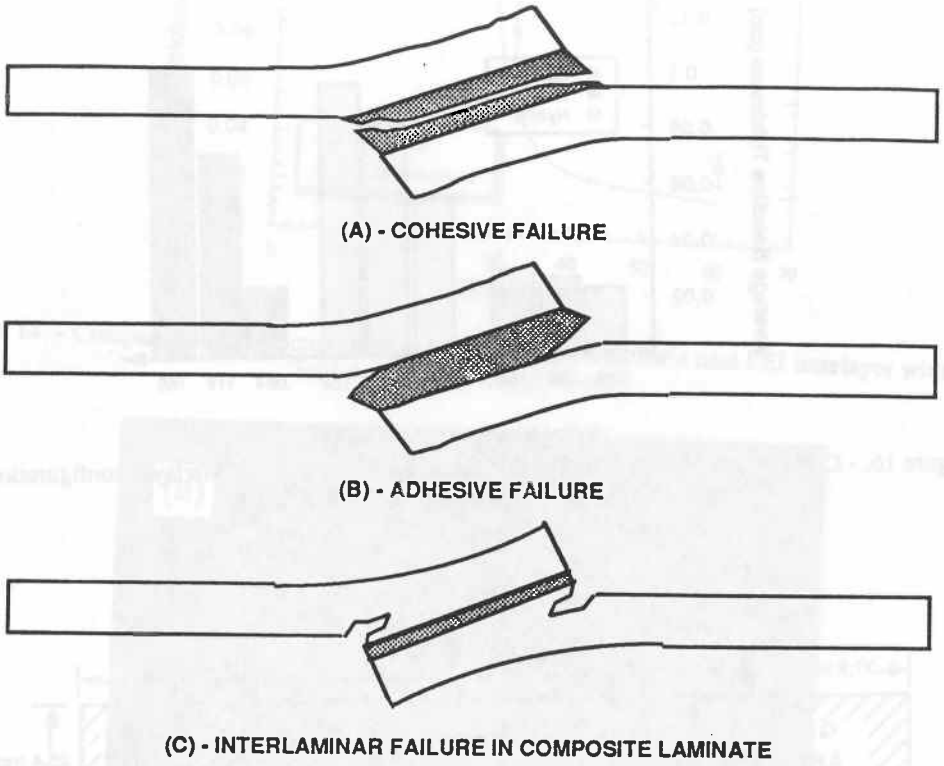

Figure 19. - Typical failure modes in single lap shear test specimen.

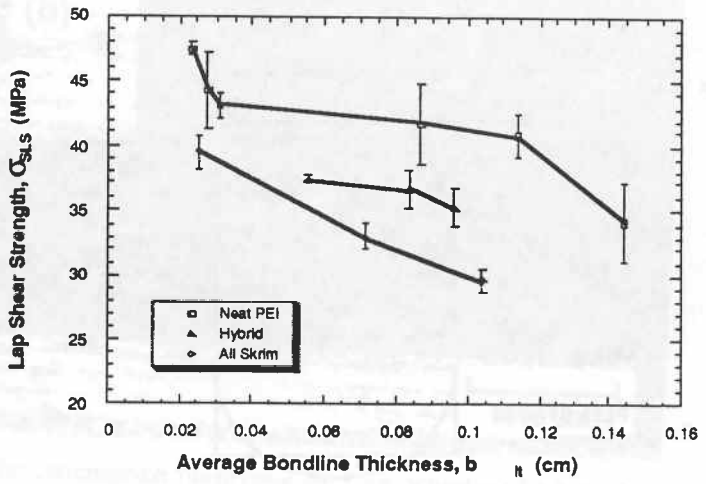

Figure 20. - Strength results as a function of bondline thickness for all panels tested.

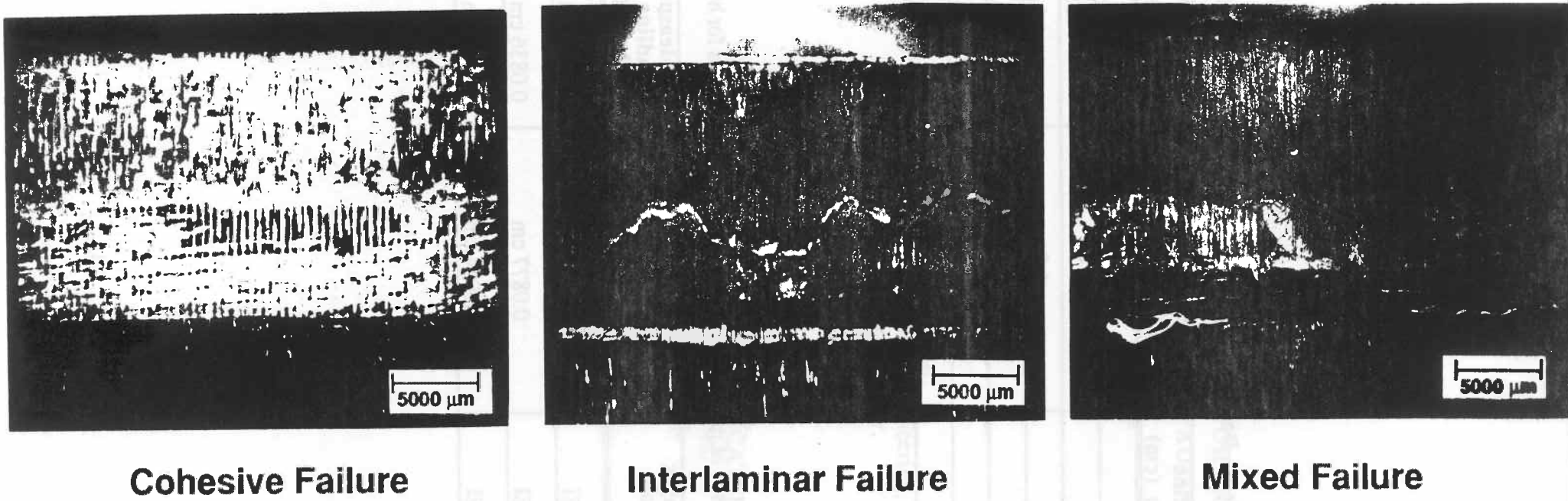

Figure 21. - Single lap shear failure mechanisms.

TABLES

Table 1. - Bondline thickness results for neat PEI interlayers.

Initial Bondline Thickness, b_{lto} (cm)	Dwell Time, t_d (min)	Final Bondline Thickness, b_{lt} (cm)
0.1524	0.0	0.0381
0.1524	2.5	0.1139
0.1524	5.0	0.0867
0.1524	30.0	0.0311
0.0889	30.0	0.0278
0.0381	30.0	0.0235

Table 2. - Comparison of predicted and actual bondline thicknesses for hybrid interlayers.

Initial Interlayer Configuration, b_{lto}	Predicted Final Bondline Thickness, b_{lt}	Measured Final Bondline Thickness, b_{lt}; (St.Dev.)
1 Skrim:2 PEI	0.0526 cm	0.0555 cm (±0.0094 cm)
3 Skrim:4 PEI	0.0877 cm	0.0836 cm (±0.0074 cm)
5 Skrim:6 PEI	0.1084 cm	0.0963 cm (±0.0105 cm)